

Isotopic effects of hydrogen adsorption in carbon nanotubes

M.C. Gordillo, J. Boronat, and J. Casulleras

*Departament de Física i Enginyeria Nuclear, Campus Nord B4-B5,
Universitat Politècnica de Catalunya. E-08034 Barcelona, Spain*

(November 1, 2018)

Abstract

We present diffusion Monte Carlo calculations of D_2 adsorbed inside a narrow carbon nanotube. The 1D D_2 equation of state is reported, and the one-dimensional character of the adsorbed D_2 is analyzed. The isotopic dependence of the constitutive properties of the quantum fluid are studied by comparing D_2 and H_2 . Quantum effects due to their different masses are observed both in the energetic and the structural properties. The influence of the interatomic potential in one-dimensional systems is also studied by comparing the properties of D_2 and 4He which have nearly the same mass but a sizeably different potential. The physics of molecular hydrogen adsorbed in the interstitial channels of a bundle of nanotubes is analyzed by means of both a diffusion Monte Carlo calculation and an approximate mean field method.

I. INTRODUCTION

Since their discovery by Iijima in 1991,¹ carbon nanotubes and their fascinating properties have attracted the attention of both theoretical and experimental physicists.²⁻⁴ Nanotubes are basically long cylinders, their walls being formed from one (single-walled carbon nanotubes, SWCN) or several (multiple-walled ones, MWCN) graphite sheets. One of its more important features is its extremely narrow width, with diameters in the nanometer scale, ranging from ~ 7 to 40 \AA , compared to its length, thousands of times larger. The enormous length to diameter ratio and the narrowness of the tube make nanotubes excellent systems to hold inside nearly perfect one-dimensional fluids. Moreover, as a consequence of its narrowness, the adsorption energy of an atom or molecule inside a carbon nanotube is several times greater than on planar graphite. This feature ensures that any particle of adequate size will be swallowed inside carbon nanotubes, provided that the half-fullerene caps at their ends are removed. Its use as a possible solution to the packing of H_2 in fuel cells has been discussed in the literature.⁵⁻⁹

Apart from its technological interest, the quasi-one dimensionality of these carbon tubes is itself an interesting property from a purely theoretical point of view. In the same way that a sheet of graphite provides an almost perfectly 2D experimental environment, the small transversal room available to the particles adsorbed in a narrow carbon nanotube creates a proper setup to extract experimental information of quasi-one-dimensional systems. Additionally, if the temperature is low enough, quantum effects become important, and an experimental realization of a quasi-one-dimensional quantum fluid is realized. A first step in that direction has been recently given by Teizel *et al.*,¹⁰ who unambiguously observed the quasi-one dimensional behaviour of ^4He adsorbed inside SWCN bundles. The helium intake could be directed either to the inside of the nanotubes, to the interstitial channels between the several tubes constituting a bundle, or to the external surface of the nanotube bundle. The occupation probability in the three regions depends on the geometry of the bundle, on the *size* of the atom/molecule to be adsorbed and, finally, on the interatomic potential between the carbon atom and each particular species.¹¹ In all cases, an almost perfect alignment of the atoms is granted. Encouraged by this experimental accessibility, some theoretical work about the adsorption of quantum liquids inside nanotubes has been carried out. The most studied case is ^4He , which has been considered both in 1D and inside a (5,5) nanotube. In the limit of zero temperature, both 1D and quasi-one-dimensional ^4He are self-bound systems, with a binding energy ranging the milikelvin scale.¹²⁻¹⁴

Molecular hydrogen inside nanotubes is also a very appealing system. In fact, the confinement of H_2 in SWCN, in the limit of zero temperature, has recently deserved theoretical work. Its mass is approximately half the ^4He one, but the hydrogen-hydrogen interatomic potential has a potential well three times deeper than the helium-helium one. This prevents the existence of a liquid phase at zero temperature in both 2D and 3D, but diffusion Monte Carlo (DMC) calculations¹⁵ have shown that it is not enough to preclude it in 1D. This result is due to the reduced number of neighbours of each atom. In fact, this liquid state could be produced also in higher dimensions when the number of molecules surrounding a particular one is artificially reduced, as in small clusters¹⁶ (3D) and in surfaces doped with the right kind of impurities¹⁷ (2D).

In the present work, the DMC method is used to study the influence of both the in-

terparticle potential and mass on the thermodynamic behavior of the isotopes of molecular hydrogen, especially H_2 and D_2 , adsorbed inside a carbon nanotube. Since the electronic structure of molecular deuterium and hydrogen is the same, the D_2 - D_2 interparticle potential is identical to the H_2 - H_2 one. This is equally true for the particle-tube interactions. Moreover, the mass of the D_2 molecule is very similar to that of a ^4He atom. Thus, by comparing the deuterium results with those for helium, the effect of the respective potential wells can be inferred. On the other hand, the influence of the zero-point energy in the thermodynamic behavior of a quasi-one dimensional array can be drawn from the comparison between the deuterium and hydrogen results. In the last part of the paper, we present results for the equation of state of H_2 , D_2 , and ^4He when they are adsorbed in the interstitial channels of a nanotube bundle. The influence of neighbouring arrays in a particular one, as a function of the interchannel separation, is studied using the DMC equation of state of purely 1D systems. The attractive Van der Waals tails between the arrays increase the binding energy of the adsorbed liquid in a quantity which decreases with the interchannel separation. Using the DMC method, it is verified that a *mean field* approximation, as suggested in Ref. 18, is very accurate at realistic separations.

The outline of the paper is as follows. In the next section, we briefly introduce the DMC algorithm used to study both the fluid adsorbed in a nanotube and the purely one-dimensional model. In Sec. III, we compare results of the equation of state and spatial structure for the two isotopes, H_2 and D_2 . Predictions for the equations of state of both isotopes, when the adsorption is in the interstitial channels, are also reported. Finally, Sec. IV comprises the summary and the main conclusions of our work.

II. METHOD

The diffusion Monte Carlo method,^{19,20} is a theoretical tool that has proved its accuracy in a large variety of systems and physical scales. It solves in a stochastic way the Schrödinger equation, providing results for the ground state which are exact for boson systems like the present one. The N -body Schrödinger equation is solved in imaginary time after the introduction of importance sampling, a standard technique to reduce the variance and make the algorithm operative. Explicitly,

$$-\frac{\partial f(\mathbf{R}, t)}{\partial t} = -D\nabla^2 f(\mathbf{R}, t) + D\nabla(\mathbf{F} f(\mathbf{R}, t)) + (E_L(\mathbf{R}) - E)f(\mathbf{R}, t), \quad (1)$$

with $f(\mathbf{R}, t) = \psi(\mathbf{R}) \Psi(\mathbf{R}, t)$, where $\psi(\mathbf{R})$ denotes a trial wave function used for importance sampling and $\Psi(\mathbf{R}, t)$ the imaginary-time-dependent wave function. In Eq. (2), $D = \hbar^2/2m$, $E_L(\mathbf{R}) = \psi(\mathbf{R})^{-1}H\psi(\mathbf{R})$ is the local energy, and $\mathbf{F}(\mathbf{R}) = 2\psi(\mathbf{R})^{-1}\nabla\psi(\mathbf{R})$ is the so-called drift force which guides the diffusion movement to regions where $\psi(\mathbf{R})$ is large.

DMC calculations have been carried out for two different situations: *i*) a pure 1D array of D_2 molecules, and *ii*) D_2 filling a tube of radius $R = 3.42 \text{ \AA}$, corresponding to the (5,5) armchair nanotube in the standard nomenclature.²¹ This structure has been chosen because it is one of the narrowest nanotubes experimentally obtained, and therefore it is expected to be close to an ideal 1D arrangement.

In the present calculation, we have considered the D_2 molecules interacting via the Silveira and Goldman (SG) pair potential.²² This semiempirical interaction is the same that has been used in Ref. 15 in the study of H_2 in tubes, and has become the standard approach in molecular hydrogen and molecular deuterium calculations. The SG interaction is a spherically averaged model, even though the pair of molecules involved are ellipsoids. However, the eccentricity of the ellipsoids is so small ($r = 0.94$, in the H_2 case) that it produces results of remarkable accuracy, even at low temperatures. For the D_2 -tube interaction we have used the Stan and Cole (SC)^{7,23} H_2 -tube interaction. This is a cylindrically averaged potential, i.e., the potential felt by a molecule inside the tube is a function only of its distance to the center of the tube. We have verified that the differences between the results obtained with this averaged interaction and the ones derived by explicitly summing up all the C- D_2 interactions inside the tube are negligible. The SC potential depends only on three parameters: σ , ϵ , and the radius of the tube. For the (5,5) tube considered, $R = 3.42 \text{ \AA}$, and the parameters σ and ϵ correspond to the Lennard-Jones C- H_2 interaction ($\sigma = 2.97 \text{ \AA}$ and $\epsilon = 42.8 \text{ K}$).²³ In Fig. 1, the H_2 -tube SC potential is displayed and compared to the ^4He potential inside the same cylinder. The two curves reflect the differences between the pair (σ , ϵ) for ^4He and H_2 ; the larger values of ϵ and σ in the case of H_2 originates a deeper well and a shorter range, respectively.

The trial wave function ψ used in the 1D system is

$$\Psi^{1D}(\mathbf{R}) = \Psi_J(\mathbf{R}) , \quad (2)$$

with $\Psi_J(\mathbf{R}) = \prod_{i<j} \exp(-0.5 (b/r_{ij})^5)$ a Jastrow wave function with a McMillan two-body correlation factor.

For the simulation of D_2 inside the tube, an additional one-body factor is introduced in order to avoid the hard core of the tube-molecule interaction,

$$\Psi^T(\mathbf{R}) = \Psi_J(\mathbf{R})\Psi_c(\mathbf{R}) , \quad (3)$$

with $\Psi_c(\mathbf{R}) = \prod_i^N \exp(-cr_i^2)$, r_i being the radial distance of the particle to the center of the cylinder.

The parameters b and c entering in Ψ_J and Ψ_c , respectively, have been determined by means of a variational Monte Carlo (VMC) optimization. Near the equilibrium density we find the optimal value $b = 3.996 \text{ \AA}$, gradually increasing with the linear density λ (at $\lambda = 0.358 \text{ \AA}^{-1}$, $b = 4.026 \text{ \AA}$). The parameter c , inversely proportional to the width of the gaussian defined in Ψ_c , has been fixed to $c = 6.392 \text{ \AA}^{-2}$ due to its negligible dependence on the density. It is worth mentioning that these parameters are different from the ones used for H_2 in the same setup¹⁵ ($b = 3.759 \text{ \AA}$, $c = 4.908 \text{ \AA}^{-2}$).

III. RESULTS

A. Low-density regime

In order to study the behavior of the several isotopes of molecular hydrogen inside nanotubes, the dependence of the adsorption energy on the mass species constitutes a first

relevant point. Since the interparticle and tube-molecule potentials do not distinguish between isotopes, their different masses play the central role. At low densities, the dominant effect is due to the binding energy of single independent molecules. From our DMC calculations the binding energy of a single molecule inside a carbon tube turns out to be, for the (5,5) tube, -1539.87 ± 0.11 K for H_2 , and -1605.23 ± 0.01 K and -1624.37 ± 0.01 K for D_2 and T_2 , respectively. The increase in the binding energy with the mass comes from the combination of two features: a decrease in the kinetic energy, mainly due to a direct effect of the mass ($m_{\text{H}_2}/m_{\text{D}_2} \simeq 1/2$, $m_{\text{D}_2}/m_{\text{T}_2} \simeq 2/3$), and a simultaneous increase of the potential energy. Although those energies correspond to the ground state of single molecules at 0 K, they constitute a very good estimation in the limit of infinite dilution at nonzero temperatures. From the above binding energies one can extract information on the selectivity in the adsorption inside the nanotube. Following Ref. 24, the selectivity of isotope 2 with respect to isotope 1 can be defined by the quotient $S = (x_1/x_2)/(y_1/y_2)$ with x_i (y_i) the nanotube (bulk) mole fractions. It has been proved that in the limit of zero pressure the selectivity S_0 is very well approximated by

$$S_0 = \frac{m_2}{m_1} \exp\left(-\frac{E_1 - E_2}{T}\right), \quad (4)$$

where E_i is the binding energy of isotope i . Considering $T = 20$ K, as in Ref. 24, we obtain $S_0(\text{T}_2/\text{H}_2) = 22.8$ and $S_0(\text{T}_2/\text{D}_2) = 1.7$ for the (5,5) tube. The selectivity is especially high in the case T_2/H_2 due to the sizeable difference in binding energies between the two isotopes, $E_{\text{T}_2} - E_{\text{H}_2} = -84.5$ K. That large selectivity, which is a purely quantum effect, has been proposed in Ref. 24 to achieve an efficient isotopic sieving.

B. One- and quasi-one-dimensional systems

The ground-state properties of an array of hydrogen molecules, in a one- and in a quasi-one-dimensional environments, have also been studied using the DMC method. In a previous work,¹⁵ we had studied the case of H_2 : the equilibrium state in 1D corresponds to a liquid phase with a density $\lambda_0 = 0.2191 \pm 0.0004 \text{ \AA}^{-1}$ and an energy per particle $(E/N)_0 = -4.834 \pm 0.007$ K. A first approach to determine the equation of state of 1D D_2 is based on the use of the average correlation approximation (ACA). This approximation, which has been widely used in the ^3He - ^4He isotopic mixture in the limit of zero ^3He concentration,^{25,26} consists in the present case in evaluating the expectation value of the Hamiltonian for D_2 using the *exact* wave function of the other isotope (H_2). Thus, the energy per particle of D_2 in ACA is given by

$$\left(\frac{E}{N}\right)_{\text{D}_2} = \left(\frac{E}{N}\right)_{\text{H}_2} + \left(\frac{m_{\text{H}_2}}{m_{\text{D}_2}} - 1\right) \left(\frac{T}{N}\right)_{\text{H}_2}, \quad (5)$$

where $(T/N)_{\text{H}_2}$ is the kinetic energy of the H_2 molecule.

ACA corresponds, obviously, to a variational estimate and thus the D_2 energies obtained from Eq. (5) are upper bounds to the exact values. Using the DMC kinetic energies of 1D H_2 reported in Table I, and the total energies published in Ref. 15, we have calculated the ACA equation of state for D_2 . The results obtained are shown in Fig. 2 and compared with

the exact solution derived from a DMC calculation of 1D D₂. Both equations of state (lines) correspond to a least squares fit to the data in the usual form

$$\frac{E}{N} = \left(\frac{E}{N}\right)_0 + A \left(\frac{\lambda - \lambda_0}{\lambda_0}\right)^2 + B \left(\frac{\lambda - \lambda_0}{\lambda_0}\right)^3. \quad (6)$$

The parameters $(E/N)_0$, λ_0 , A , and B are given in Table II. The upper bounds provided by ACA appear clearly reflected in Fig. 2, its *quality* being quite reasonable taking into account its straightforward estimation (5). In fact, the discrepancies between ACA and the exact results are less than 2 % for the equilibrium density value, and around 3 % for the binding energies. ACA can also be used to estimate the equation of state of the T₂ fluid, a system that we have not studied here using the explicit DMC calculation. For 1D T₂, ACA predicts $\lambda_0 = 0.2501 \text{ \AA}^{-1}$ and $(E/N)_0 = -12.677 \text{ K}$.

On the other hand, the equation of state of D₂ inside a tube can also be estimated by ACA, since the tube-molecule SC potential does not depend on the particular isotope. Using the H₂ equation of state (Ref. 15) and the H₂ kinetic energies reported in Table I, the ACA results compare with the corresponding DMC ones with an accuracy similar to the 1D case. DMC energy results for both 1D D₂ and D₂ adsorbed in the (5,5) nanotube are displayed in Fig. 3. In order to show the two equations of state with the same energy scale, we have subtracted to the tube results the adsorption energy of a single molecule. In Fig. 3, the curves are polynomial fits (6) to the DMC data, the optimal parameters for the tube being reported in Table II. It can be seen that the equilibrium density for 1D D₂ and D₂ adsorbed in the (5,5) nanotube are almost identical. This is also true for the location of the spinodal points of D₂, $\lambda_s^{1D} = 0.230 \pm 0.001 \text{ \AA}^{-1}$ and $\lambda_s^T = 0.232 \pm 0.001 \text{ \AA}^{-1}$, which can be derived from the data contained in Table II.

The binding energies, in the respective equilibrium points $((E/N)_0)$, are slightly different: the additional transverse degree of freedom only amounts to an increase of 0.091 K. This increase in the binding energy is nearly a factor two smaller than the one drawn from the DMC calculations for H₂ (0.172 K). In relative terms, the increase of the binding energy is only a 0.85 % for D₂ versus a 3.5 % for H₂. Therefore, one can conclude that the effects of the additional degree of freedom of the D₂ molecules in the radial direction inside the nanotube, which account for the enhancement of the binding energy, are reduced by the greater mass of the D₂ molecule with respect to the H₂ one. As a matter of comparison, it is illustrative to compare the effects observed in D₂ with the ones previously studied in ⁴He using the same methodology and geometry. It is worth noticing that the masses of D₂ and ⁴He are nearly the same whereas the interatomic potentials are sizeably different. The DMC results show that the latter effect is completely determinant: in ⁴He the relative difference mentioned above is 90 %, two orders of magnitude larger than in D₂. Another minor effect that contributes to the one-dimensionality of molecular deuterium adsorbed inside the tube, is the larger hard-core size of the C-D₂ interaction ($\sigma_{C-D_2} = 2.97 \text{ \AA}$), versus the C-He one ($\sigma_{C-He} = 2.74 \text{ \AA}$). The mass versus potential effects can also be seen in the value of the equilibrium density. Inside the tube, λ_0 goes from $0.079 \pm 0.003 \text{ \AA}^{-1}$ in ⁴He, to $0.2200 \pm 0.0006 \text{ \AA}^{-1}$ in H₂, to reach $0.2473 \pm 0.0002 \text{ \AA}^{-1}$ in D₂. That sequence clearly indicates that the main influence in λ_0 comes from the potential, since the isotopic change varies the location of the energy minimum less than 15 %. Most probably, the features observed in these systems have a more general character and one can guess that if the well

of the interatomic potential is increased and/or the mass of the particle adsorbed inside a tube is enlarged, the effect would be an increase in the λ_0 value.

In Fig. 4, the density dependence of the pressure for both 1D D_2 and D_2 inside the tube is reported from the equilibrium density up to 0.30 \AA^{-1} . For the sake of comparison, the same results for H_2 are also plotted. In both H_2 and D_2 , the pressures for the 1D systems (solid lines) are greater than the ones for the tubes (dashed lines) at the same λ , the difference being quite similar for the two isotopes. For the same geometry and at equal density, the pressure of H_2 is always larger, a fact that is basically due to its slightly smaller equilibrium density.

Complementary and useful information on the system can be obtained from the microscopic study of the spatial structure of the molecules in the array. In Fig. 5 the radial distribution functions, $g_z(r)$, along the z axis, are shown. They correspond to the quantum fluids adsorbed in the tube at their respective equilibrium densities λ_0 . The 1D counterparts are nearly identical and are not displayed. Being the denser of the three systems, D_2 exhibits accordingly the most pronounced oscillations in the $g_z(r)$ function. The shift in the positions of the maxima for the two molecular isotopes arises basically from the difference in their respective λ_0 's. A comparison of the radial distributions of H_2 and D_2 at the same linear density, not shown for simplicity, indicates so. In the ^4He case, the much lower equilibrium density, direct consequence of the different potential, explains the smoothness of the $g_z(r)$ obtained.

The radial densities inside the (5,5) tube have been also studied. In Fig. 6, the radial densities for ^4He , H_2 , and D_2 for the same linear density $\lambda = 0.245 \text{ \AA}^{-1}$ are shown. The trends shown in the figure are common to all densities studied: the particle with the largest mass (D_2) is the one which spends more time in regions closer to the center of the tube, i.e., D_2 in the tube is the closest to a one-dimensional system. The change in the mass and in the interatomic potential work in the same direction: the radial densities of H_2 and ^4He are quite similar. Both curves show a decrease in the radial localization and larger fluctuations in the transverse direction.

C. Adsorption in a bundle of nanotubes

The absorption of different species inside the interstitial channels of bundles, formed when several nanotubes are staked together, has been theoretically predicted¹¹ and experimentally observed.¹⁰ The staking of the nanotubes allows for the formation of an hexagonal network of quasi-one dimensional channels separated by distances which depend on the diameter of the nanotubes themselves. For instance, when the nanotube ropes are made out of (5,5) constituents, the distance between two adjacent tubes is 10.26 \AA , whereas the closest interstitial channels are located $\sim 5.9 \text{ \AA}$ apart. The interstitial channels are very narrow, with effective diameters oscillating between 3 and 3.5 \AA .²⁷ This size is considerably smaller than the diameter (6.8 \AA) of the (5,5) tube considered in the previous subsection. Therefore, it is plausible to assume that if molecular hydrogen or deuterium is introduced inside one of this channels, its behavior would have even a more one dimensional character than in the inner part of a single tube.

Considering the previous arguments, a quantum fluid adsorbed in the intersites can be well modelled by hexagonal arrangements of purely 1D systems, mutually separated by the

real interchannel distance in the bundle. To a large extent, the additional consideration of the interactions between the adsorbed atoms/molecules and the carbon atoms of the nanotube walls would simply introduce a constant shift in the energy scale. The influence of neighbouring channels in the binding energy of ^4He adsorbed in one of them has been estimated in Ref. 18 considering a *mean field* approximation. In this approach, the neighbouring channels are seen as uniform arrays that only contribute to increase the potential energy in the form

$$\Delta_{\text{mf}} = \frac{\lambda}{2} \int_{-\infty}^{\infty} dx V(\sqrt{x^2 + d^2}) , \quad (7)$$

where d is the distance between the reference channel and one of its neighbours. The total energy correction is obtained by summing up the contribution of the nearest neighbours, the next-nearest neighbours, and then on up to a desired accuracy. From its definition (7) it is clear that the energy per particle in this approximation,

$$E/N = (E/N)_{\text{1D}} + \Delta_{\text{mf}} , \quad (8)$$

is an upper bound to the exact energy.

In order to test the *mean field* approximation (8), we have performed full DMC calculations of a system formed by an hexagonal array of 1D H_2 channels. Since the distances between channels depend on the diameter of the tubes, the calculations have been made in the more challenging case for Eq. (8), a bundle of (5,5) nanotubes. That tube is one of the narrowest experimentally obtained, and therefore the interchannel distance is one of the smallest in nature. Actually, that is an unrealistic case since the corresponding interstitial channels are too narrow to adsorb H_2 . The DMC energies are displayed in Fig. 7, and compared with the approximated estimations (8). As it is evident in the figure, both results are nearly identical, at least in the density range considered. The conclusion is that correlations between hydrogen molecules located in different channels suppose a negligible contribution to the energy, even in this case where the channels are very close. In Fig. 7, there is also reported the equation of state of 1D H_2 . As one can see, the increase of the binding energy of the system, when the array is immersed in a bundle, is as large as a factor two.

Having checked the validity of the *mean field* approach (8) in an exigent case, one can use that approximation to study the equation of state of molecular hydrogen and helium adsorbed in other more appropriate bundles. It is worth mentioning that the number of neighbours to be included in Δ_{mf} has to be larger than ten, otherwise the binding energy is underestimated in a 5 %. Besides the (5,5) bundle, with an interchannel distance $a = 5.92 \text{ \AA}$, we have analyzed the following cases: (6,6), $a = 6.71 \text{ \AA}$; (8,8), $a = 8.27 \text{ \AA}$; (10,10), $a = 9.83 \text{ \AA}$. The fluids that have been analyzed are ^4He , D_2 , and H_2 . In Fig. 8, the differences between the equilibrium density in the bundles and in the purely 1D system are shown for the three cases. There is a clear difference (an order of magnitude) between the increase of λ_0 , when ^4He is adsorbed in the intersites, and the density shift experimented by the two hydrogen isotopes. In H_2 and D_2 the change in density is small but one can distinguish a slightly larger effect in the lighter isotope. In all cases, the density difference decreases when the interchannel separation increases. However, H_2 and D_2 have already reached the 1D equilibrium density in the (10,10) geometry whereas ^4He still shows a sizeable effect.

The increase of the binding energies with respect to the one-dimensional systems are reported in Fig. 9. The different points correspond to the same bundles reported in Fig. 8.

In absolute terms, that increase is much larger in molecular hydrogen than in ^4He , the effect being slightly larger in D_2 than in H_2 for all the bundles. The energy difference between H_2 and D_2 is very small and decreases when the interchannel distance increases. It is clear, from the *mean field* correction (7), that the difference in energy between the two isotopes arises from their different densities since the interatomic potential is the same. In ^4He the shift in energy is comparatively small but, taking into account that the 1D ^4He binding energy¹³ is only $(E/N)_0 = -0.0036$ K, one concludes that the bundle effects are much larger in ^4He than in molecular hydrogen.

IV. SUMMARY AND CONCLUSIONS

In this work, we have studied the zero-temperature equation of state of molecular deuterium, and compared the results with those previously obtained¹³ for ^4He and molecular hydrogen.¹⁵ The results show that the different masses of the two isotopes do influence both the energetic and structural properties. As a general trend, D_2 appears as a slightly denser liquid, a fact that is observed in its equation of state and also in the radial distribution functions. The comparison between D_2 and ^4He , two *particles* with the same mass but with very different interatomic potentials, has shed light on the influence of the potential in one-dimensional systems. Concerning the mass and potential changes, the DMC results show unambiguously that the potential effects are manifestly dominant. Bundles of carbon nanotubes have also been studied by modelling them as hexagonal one-dimensional arrays. The explicit DMC calculation of the system has allowed to check the accuracy of a previously suggested *mean field* approximation.¹⁸ Once verified the validity of that approximation, we have analyzed the effects of the neighbouring channels on the 1D equation of state. Our results show that those effects are much more relevant in ^4He than in molecular hydrogen.

In the tube and bundle calculations, we have assumed that the interparticle potential is not modified by the existence of nearby carbon atoms. Recently, Cole and coworkers^{28,29} have estimated the effective correction in the two-body potential due to three-body interactions between two particles and the carbon atoms of the nanotube wall. This three-body interaction has been modelled by the well-known triple-dipole interaction derived by Axilrod and Teller,³⁰ a potential energy contribution that is mostly repulsive. In the case of molecular hydrogen in the interstitial channels, the well of the effective Silvera and Goldman potential is reduced by approximately a factor two. This unexpected and big effect would modify some of the results presented in our work. Nevertheless, it is well-known that, in spite of the fact that Axilrod-Teller is the dominant contribution to V_3 , at short interparticle distances an attractive force emerges. This short-ranged three-body interaction, known as exchange interaction,³¹ is due to the influence of a third particle in the charge densities of two interacting atoms. Due to the short interparticle distances $\text{H}_2\text{-C-H}_2$ in the channel, that attractive term would partially cancel the repulsion introduced by Axilrod-Teller. We have preferred to ignore the three-body corrections³² until a better knowledge of the nonadditive terms of this particular system is achieved.

We plan, in the near future, to introduce in the simulation the possibility of the swelling of the channels when molecular hydrogen is adsorbed. The aim would be to test, by a microscopic calculation, the recent theoretical result³³ that H_2 forces the nanotube bundles to slightly spread upon adsorption. We hope our calculations, and the ones carried out by

other theoretical groups, can stimulate new experiments on molecular hydrogen adsorption in carbon nanotubes and bundles, especially at low-temperature where quantum effects become macroscopic.

ACKNOWLEDGMENTS

The authors gratefully acknowledge Prof. M. W. Cole for stimulating discussions. This research has been partially supported by DGEIC (Spain) Grant N^o PB98-0922, and DGR (Catalunya) Grant N^o 1999SGR-00146. M. C. G. thanks the Spanish Ministry of Education and Culture (MEC) for a postgraduate contract. We also acknowledge the supercomputer facilities provided by the CEPBA.

REFERENCES

- ¹ S. Iijima, *Nature* **354**, 56 (1991).
- ² R. Saito, G. Dresselhaus, and M. S. Dresselhaus, *Physical Properties of Carbon Nanotubes* (Imperial College Press, London, 1998).
- ³ M. S. Dresselhaus, G. Dresselhaus, P. C. Eklund, and R. Saito, *Phys. World* **11**, 33 (1998).
- ⁴ P. M. Ajayan and T. W. Ebbesen, *Rep. Prog. Phys.* **60**, 1025 (1997).
- ⁵ A. C. Dillon, K. M. Jones, T. A. Bekkedahl, C. H. Kiang, D. S. Bethune, and M. J. Heben, *Nature* **386**, 377 (1997).
- ⁶ F. Darkrim and D. Levesque, *J. Chem. Phys.* **109**, 4981 (1998).
- ⁷ G. Stan and M. W. Cole, *J. Low Temp. Phys.* **110**, 539 (1998).
- ⁸ M. Rzepka, P. Lamp, M. A. de la Casa-Lillo, *J. Phys. Chem. B* **102**, 10894 (1998).
- ⁹ Q. Wang and J. K. Johnson, *J. Chem. Phys.* **110**, 577 (1999).
- ¹⁰ W. Teizer, R. B. Hallock, E. Dujardin, and T. W. Ebbesen, *Phys. Rev. Lett.* **82**, 5305 (1999); *Phys. Rev. Lett.* **84**, 1844 (2000).
- ¹¹ G. Stan, M. J. Bojan, S. Curtarolo, S. M. Gatica, and M. W. Cole, <http://arXiv.org/abs/cond-mat/0001334>.
- ¹² E. Krotscheck and M. D. Miller, *Phys. Rev. B* **60**, 13038 (1999).
- ¹³ M. C. Gordillo, J. Boronat, and J. Casulleras, *Phys. Rev. B* **61**, R878 (2000).
- ¹⁴ M. Boninsegni and S. Moroni, *J. Low Temp. Phys.* **118**, 1 (2000).
- ¹⁵ M. C. Gordillo, J. Boronat, and J. Casulleras, *Phys. Rev. Lett.* **85**, 2348 (2000).
- ¹⁶ P. Sindzingre, D. M. Ceperley, and M. L. Klein, *Phys. Rev. Lett.* **67**, 1871 (1991).
- ¹⁷ M. C. Gordillo and D. M. Ceperley, *Phys. Rev. Lett.* **79**, 3010 (1997).
- ¹⁸ M. W. Cole, V. H. Crespi, G. Stan, C. Ebner, J. M. Hartman, S. Moroni, and M. Boninsegni. *Phys. Rev. Lett.* **84**, 3883 (2000).
- ¹⁹ B. L. Hammond, W. A. Lester Jr., and P. J. Reynolds, *Monte Carlo Methods in Ab Initio Quantum Chemistry* (World Scientific, Singapore, 1994).
- ²⁰ J. Boronat and J. Casulleras, *Phys. Rev. B* **49**, 8920 (1994).
- ²¹ S. Iijima and T. Ichihashi, *Nature* **363**, 603 (1993).
- ²² I. F. Silvera and V. V. Goldman, *J. Chem. Phys.* **69**, 4209 (1978).
- ²³ G. Stan and M. W. Cole, *J. Low Temp. Phys.* **110**, 539 (1998).
- ²⁴ Q. Wang, S. R. Challa, D. S. Sholl, and J. K. Johnson, *Phys. Rev. Lett.* **82**, 956 (1999).
- ²⁵ G. Baym, *Phys. Rev. Lett.* **17**, 952 (1966).
- ²⁶ J. Boronat, A. Fabrocini, and A. Polls, *J. Low Temp. Phys.* **74**, 347 (1989).
- ²⁷ J. Tersoff and R. S. Ruoff, *Phys. Rev. Lett.* **73**, 676 (1994).
- ²⁸ M. K. Kostov, M. W. Cole, J. C. Lewis, P. Diep, and J. K. Johnson, *Chem. Phys. Lett.* **332**, 26 (2000).
- ²⁹ M. K. Kostov, J. C. Lewis, and M. W. Cole, to appear in *Many-Body Theories XXV*, edited by S. Hernández; <http://arXiv.org/abs/cond-mat/0010015>.
- ³⁰ B. M. Axilrod and E. Teller, *J. Chem. Phys.* **11**, 299 (1943).
- ³¹ L. W. Bruch and I. J. McGee, *J. Chem. Phys.* **59**, 409 (1973).
- ³² In Ref. 20, the contribution of several three-body potentials to the equation of state of liquid ^4He is calculated and discussed.
- ³³ M. M. Calbi, F. Toigo, and M. W. Cole, <http://arXiv.org/abs/cond-mat/0011509>.

TABLES

λ (\AA^{-1})	1D		Tube	
	H ₂	D ₂	H ₂	D ₂
0.225	9.36 ± 0.03	5.63 ± 0.02	125.5 ± 0.2	80.5 ± 0.1
0.230	10.20 ± 0.03	6.03 ± 0.02	125.8 ± 0.2	80.9 ± 0.1
0.235	11.32 ± 0.02	6.57 ± 0.02	127.1 ± 0.2	81.2 ± 0.1
0.239	12.30 ± 0.03	7.28 ± 0.02	127.8 ± 0.2	81.8 ± 0.1
0.259	18.27 ± 0.05	10.98 ± 0.03	133.6 ± 0.2	85.4 ± 0.1

TABLE I. Kinetic energies of H₂ and D₂ in 1D and inside a (5,5) carbon nanotube.

	ACA	1D D ₂	D ₂ in a tube
λ_0 (\AA^{-1})	0.2419 ± 0.0007	0.2457 ± 0.0003	0.2473 ± 0.0002
$(E/N)_0$ (K)	-10.282 ± 0.008	-10.622 ± 0.016	-1615.94 ± 0.015
A (K)	154 ± 3	$2.0 \cdot 10^2 \pm 1.0 \cdot 10^1$	$2.13 \cdot 10^2 \pm 1.0 \cdot 10^1$
B (K)	$4.5 \cdot 10^2 \pm 70$	$9.6 \cdot 10^2 \pm 1.2 \cdot 10^2$	$1.10 \cdot 10^3 \pm 1.1 \cdot 10^2$

TABLE II. Parameters of the equation of state of D₂ (Eq. 6).

FIGURES

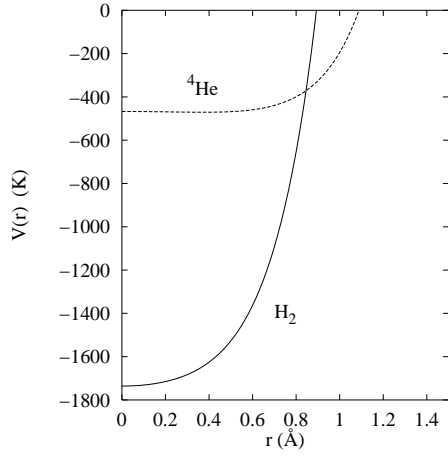


FIG. 1. SC tube-molecule/atom potentials inside a (5,5) carbon nanotube.

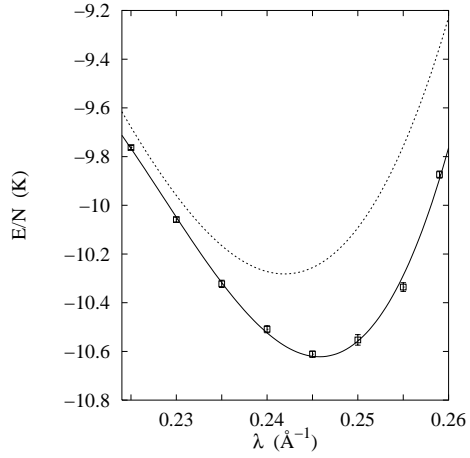


FIG. 2. Equation of state of 1D D_2 . The symbols are the DMC energies and the solid line a polynomial fit to them (6). The dashed line corresponds to the energies estimated using ACA.

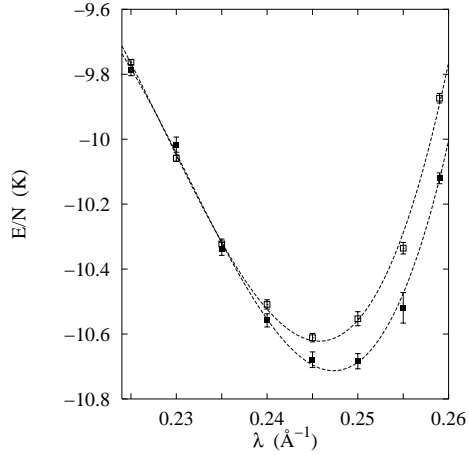


FIG. 3. Comparison between the equation of state of 1D D_2 and D_2 adsorbed in the nanotube. Filled squares correspond to the tube results; open squares, to the 1D ones. The lines are polynomial fits to the DMC data. To better compare both results, we have subtracted to the tube energies the binding energy of a single molecule.

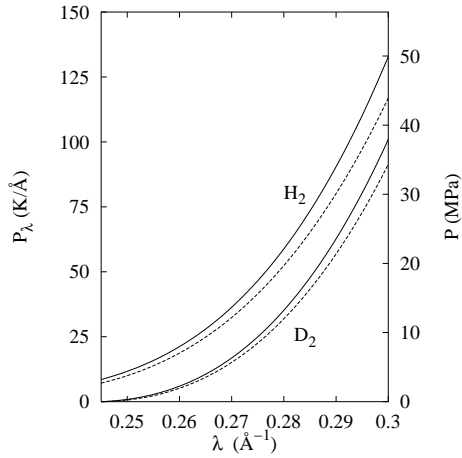


FIG. 4. Pressure of D_2 and H_2 as a function of the linear density λ . Solid and dashed lines correspond to the 1D and nanotube systems, respectively. The left (right) scale is the 1D (nanotube) pressure.

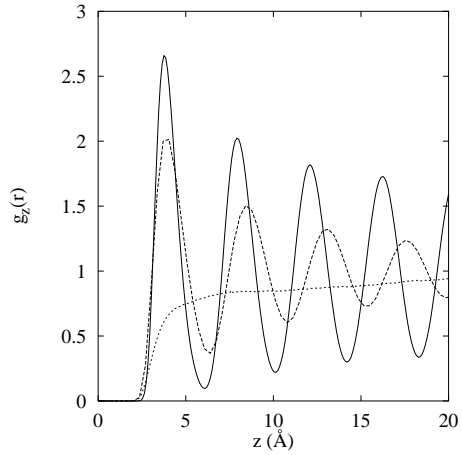


FIG. 5. Two-body distribution function in the nanotube system, and in the z direction. Solid, dashed, and dotted lines correspond to D_2 , H_2 , and ${}^4\text{He}$, respectively. All curves are calculated at their respective equilibrium densities λ_0 .

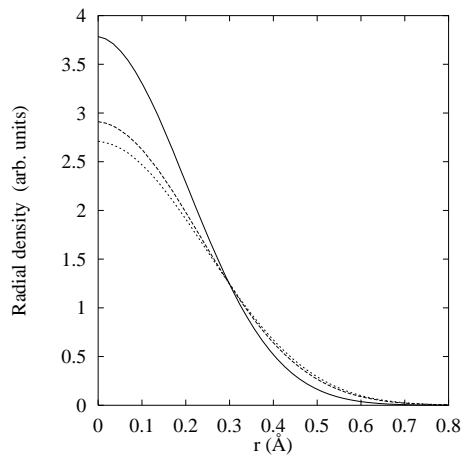


FIG. 6. Radial density of D_2 (solid line), H_2 (dashed line), and ${}^4\text{He}$ (dotted line) inside the (5,5) nanotube.

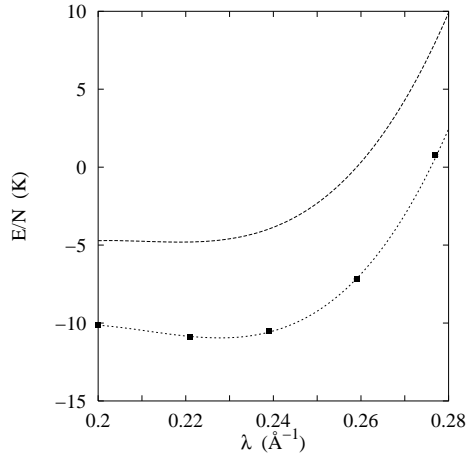


FIG. 7. Equation of state of D_2 in a bundle of (5,5) nanotubes. The symbols are the DMC results, and the dotted line corresponds to the mean field approximation. The dashed line is the 1D result.

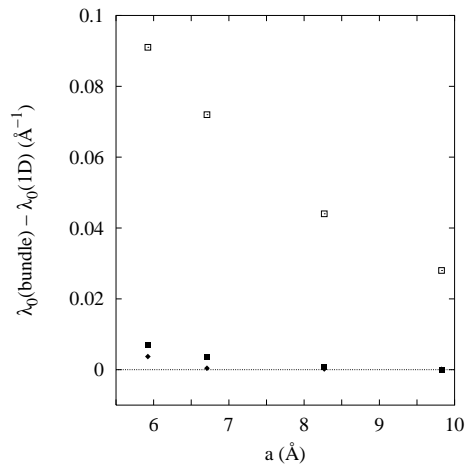


FIG. 8. Difference between the equilibrium densities, in a bundle and in a 1D array, as a function of the cell parameter a . Diamonds, filled squares, and open squares correspond to D_2 , H_2 , and ^4He , respectively.

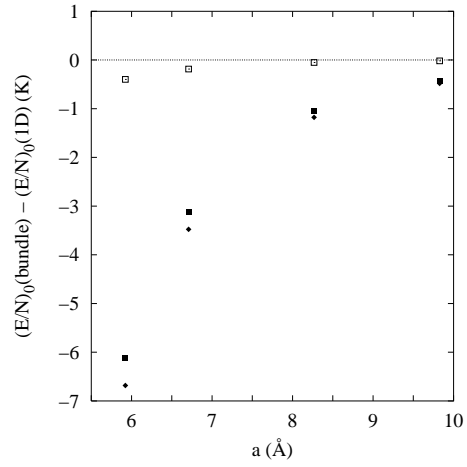


FIG. 9. Difference between the binding energies, in a bundle and in a 1D array, as a function of the cell parameter a . Diamonds, filled squares, and open squares correspond to D_2 , H_2 , and ${}^4\text{He}$, respectively.